ARMY RESEARCH LABORATORY

Exploiting Unique Features of Nanodiamonds as an Advanced Energy Source

**by William D. Mattson, Radhakrishnan Balu,
Betsy M. Rice, and Jennifer A. Ciezak**

ARL-TR-4783 **April 2009**

NOTICES

Disclaimers

The findings in this report are not to be construed as an official Department of the Army position unless so designated by other authorized documents.

Citation of manufacturer's or trade names does not constitute an official endorsement or approval of the use thereof.

Destroy this report when it is no longer needed. Do not return it to the originator.

Army Research Laboratory
Aberdeen Proving Ground, MD 21005-5069

ARL-TR-4783 **April 2009**

Exploiting Unique Features of Nanodiamonds as an Advanced Energy Source

William D. Mattson, Radhakrishnan Balu,
Betsy M. Rice, and Jennifer A. Ciezak
Weapons and Materials Research Directorate, ARL

REPORT DOCUMENTATION PAGE

Form Approved
OMB No. 0704-0188

PLEASE DO NOT RETURN YOUR FORM TO THE ABOVE ADDRESS.

1. REPORT DATE *(DD-MM-YYYY)*	2. REPORT TYPE	3. DATES COVERED (From - To)
April 2009		FY08

4. TITLE AND SUBTITLE

Exploiting Unique Features of Nanodiamonds as an Advanced Energy Source

5a. CONTRACT NUMBER

5b. GRANT NUMBER

5c. PROGRAM ELEMENT NUMBER

6. AUTHOR(S)

William D. Mattson, Radhakirshnan Balu, Betsy M. Rice, and Jennifer A. Ciezak

5d. PROJECT NUMBER

5e. TASK NUMBER

5f. WORK UNIT NUMBER

7. PERFORMING ORGANIZATION NAME(S) AND ADDRESS(ES)

U.S. Army Research Laboratory
ATTN: AMSRD-ARL-WM-BD
Aberdeen Proving Ground, MD 21005-5069

8. PERFORMING ORGANIZATION REPORT NUMBER

ARL-TR-4783

9. SPONSORING/MONITORING AGENCY NAME(S) AND ADDRESS(ES)

10. SPONSOR/MONITOR'S ACRONYM(S)

11. SPONSOR/MONITOR'S REPORT NUMBER(S)

12. DISTRIBUTION/AVAILABILITY STATEMENT

Approved for public release; distribution unlimited.

13. SUPPLEMENTARY NOTES

14. ABSTRACT

We present a combined experimental and theoretical study on carbon nanodiamonds (NDs) using Raman and DAC experimentation and *ab initio* calculations. Our calculations confirm the surface reconstruction to a fullerene-like structure, and indicate compression of the diamond core, producing an estimated internal pressure of 50 GPa. Quantum molecular dynamics simulations of hypervelocity collisions of NDs show that upon collision, shock-induced amorphization first occurs, followed by complete disruption of the ND surface and ejection of reactive particles into the vacuum. Raman spectra of oxidized ND samples at increasing pressures showed a subtle increase in the vibrational intensity of the Raman feature centered near 1335 cm^{-1} near 18 GPa and continued under subsequent pressure increases. The intensification of this vibrational feature is consistent with a thinning of the amorphous carbon outer shell, which results in greater exposure to the diamond core with increasing pressure and may be a precursor to Structural Bond Energy Release (SBER) initiation. Additionally, a nearly two-fold increase in the vibrational intensity of the sp^2 graphite peak centered near 1630 cm^{-1} in the spectra of the oxidized nanodiamond sample suggests the possibility of a sluggish partial phase transition from sp^3 hybridized diamond to sp^2 hybridized graphite.

15. SUBJECT TERMS

Nanodiamond high pressure SBER

16. SECURITY CLASSIFICATION OF:			17. LIMITATION OF ABSTRACT	18. NUMBER OF PAGES	19a. NAME OF RESPONSIBLE PERSON
a. REPORT	b. ABSTRACT	c. THIS PAGE			William D. Mattson
Unclassified	Unclassified	Unclassified	UU	20	19b. TELEPHONE NUMBER (*Include area code*) (410) 306-1903

Standard Form 298 (Rev. 8/98)
Prescribed by ANSI Std. Z39.18

Contents

List of Figures

Acknowledgments

This work was supported in part by the Department of Defense (DoD) High Performance Challenge Project C2L, and the 2008 U.S. Army Research Laboratory (ARL) Director's Research Initiative. All calculations were performed at the DoD Major Shared Resource Centers located at ARL and the Air Force Research Laboratory.

INTENTIONALLY LEFT BLANK

1. Objective

For the past several years, our group has been exploring materials in which energy can be trapped in metastable states, in an attempt to understand a phenomenon termed Structural Bond Energy Release (SBER). The SBER concept originated with experiments conducted in the U.S. in the 1930s by Bridgman (*1*), in which various inert common materials, such as chalk and sugar, were compressed in a Bridgman anvil cell and subjected to shear. For several materials, the combination of pressure and shear resulted in a rapid liberation of energy. These experiments generated intense interest in the former Soviet Union (FSU) (*2, 3*), yet were virtually ignored by the rest of global scientific community. Since researchers in the FSU had a particular interest in carbon, we performed theoretical calculations to characterize high-pressure states (> 600 GPa) of this potential SBER material. We initially began searching for features in the phase diagrams of carbon that would suggest sharp thresholds for shock-induced polymorphic phase transition; our calculations began with the shock Hugoniot of diamond to investigate the existence of possible anomalies that could result in the identification of new, high-pressure metastable phases of carbon. However, no such anomalies were identified.

During the course of the earlier theoretical investigation, however, we became aware of a combined experimental/theoretical study on surface reconstructions in nanodiamonds (NDs) (*4*) that suggest such crystallites might contain significant SBE. The theoretical portion of this study used semi-empirical tight binding to predict the equilibrium structure of ND; the results indicated that surface reconstruction of ND of various sizes from 1.2 to 3.0 nm occurred, in which the surface atoms repositioned themselves into fullerene-type geometrical arrangements spontaneously at low temperatures. Both the experimental and theoretical results support the existence of these "bucky diamonds, i.e., carbon nanoparticles with a diamond core of a few nanometers and a fullerene-like surface structure" (*4*). The calculations revealed tensile stress on the core of the nanocluster, implying that the reconfiguration of the fullerene-like surface compresses the diamond core. Our own calculations of the diamond shock Hugoniot (*5*) indicate that very small degrees of compression produce huge increases in pressure. Thus, any subtle changes in the bonding structure of the outer shell that produce minor bond length modifications within the ND core could generate significant stored structural bond energy within the ND. In addition to the structural strain within the core, the interfacial strain between the fullerene-type shell and the diamond core may contribute to the total stored structural energy. These findings suggest the SBER potential of bucky diamonds, in that a sudden disruption of the shell and subsequent relaxation of the internal pressure of the core might result in the destruction of the diamond structure with an accompanying energy release. To explore this possibility, a joint experimental/quantum mechanical study investigated the feasibility of SBER phenomenon in ND.

2. Approach

2.1 Experimental

Piston-cylinder type diamond anvil cells with 300 μm diamond culets were used for all static high-pressure experiments. Raw (NB-90) and Oxidized (NB90-OX) nanodiamond suspensions, were obtained from NanoBlox, Inc. The suspensions were dried in a drying oven at 150 °C over the course of several days and then ground into a fine powder. A 60–100 μm ND sample was loaded into the sample well (~120 μm in diameter) of a rhenium gasket. The pressure within the diamond anvil cell was determined from the frequency shift of the ruby R_1 fluorescence line (*6*). Raman spectra were obtained from an Ar^+ ion laser operating at 514.5 nm with an optical system previously described (*7*), and a laser spot diameter of ~4 μm at room temperature. Prior to any experimental measurements, a wavelength calibration of the spectrograph was performed with a Neon lamp; this method of calibration has an accuracy of ±1 cm^{-1}. The spectral resolution for all Raman measurements was ±4 cm^{-1}.

2.2 Theoretical

For all calculations, the PBE form of the Generalized Gradient Approximation (GGA) of the Density Functional Theory (DFT) as implemented in the local orbital basis code CP2K was used. We employed a Gaussian basis and an auxiliary plane wave basis with the kinetic energy cutoff of 400 Rydberg. All the calculations were performed at the Γ points of the Brillouin zone, as the unit cells were quite large. The SCF convergence tolerance at each step of the Quantum Molecular Dynamics (QMD) calculations for all systems studied was 1×10^{-5} a.u. Each ND was composed of 2052 atoms, and an initial optimized geometry was obtained by cleaving a sphere out of the bulk diamond with a diameter of 2.6 nm. The ND was allowed to relax in QMD simulations in the microcanonical (NVT) ensemble (T=300 K) in a simulation cell with edge length of 121.5 bohr. The reference system propagator algorithms (RESPA) implementation of the NVT ensemble implemented in CP2K was employed for the simulations of the collisions. Trajectories of the collisions were performed using a step size of 1 fs. In order to simulate a hypervelocity collision, atomic velocities for the colliding ND were assigned velocities above thermal to correspond to 10 km/s, allowing for a 20 km/s relative collision velocity. Only off-center collisions were explored.

3. Results

3.1 Experimental

The Raman spectra of the Raw (RND) and Oxidized (OND) on isothermal compression ambient to 53 GPa are shown in Figure 1 (left and right frames, respectively). Although there are similarities between the Raman spectra of the bulk single crystal (SC) diamond and micro/nanodiamond, the finite particle size of the ND results in obvious spectroscopic differences, such as shifts in the vibrational frequencies and a generalized broadening of the bands (*8*, *9*). These differences are readily apparent in figure 1 where the sharp feature near 1330 cm^{-1} arises from the first order scattering from the diamond (single crystal) anvils, and the remaining weak, broad features arise from the nanodiamonds. The Raman spectra of both ND samples show the appearance of a broad shoulder (~1260 cm^{-1}) on the low frequency side of the 1335 cm^{-1} SC feature near 15 GPa. Previous studies have shown that the vibrational position of this shoulder lies within the spectral range associated with the partial density of states of the diamond lattice, and indicates that the ND particles have a composite structure consisting of a diamond core and an amorphous carbon shell (*10*). At pressures near 15 GPa, the feature appears more intense in the RND, but with increasing pressure, the intensity in the corresponding OND spectra increases nearly two fold. The increase in the intensity of the OND feature is consistent with a thinner amorphous carbon surface structure, which would then expose the diamond core as pressure increases. An increase in the amount of exposed core is expected to be a precursor to an SBER event.

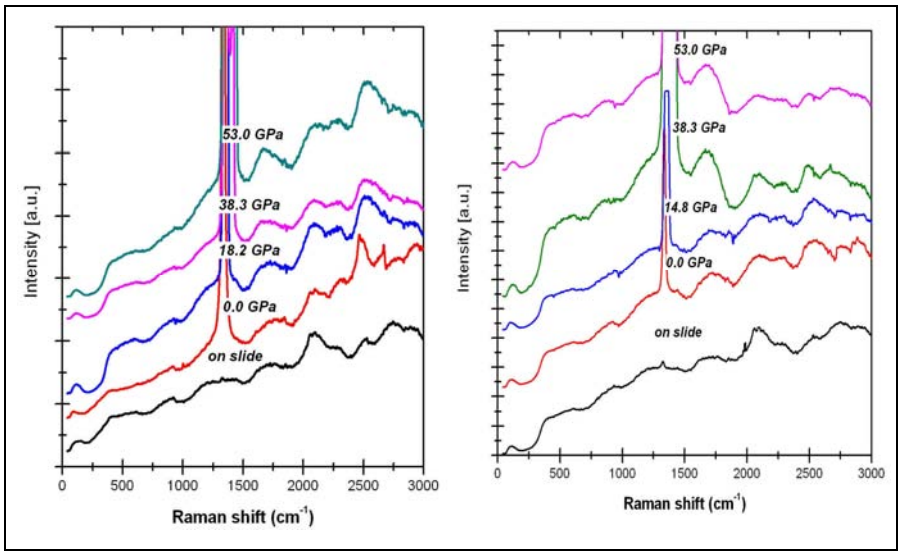

Figure 1. Raman spectra of raw (left) and oxidized (right) nanodiamonds as a function of pressure.

Note: Spectra are offset for viewing ease.

In addition to the sp^3 diamond feature, two very broad bands near 1000 cm^{-1}, and between 1500 cm^{-1} and 1800 cm^{-1}, are observed in the Raman spectra of both samples. The broad band between 1500 cm^{-1} and 1800 cm^{-1} can be interpreted as a superposition of two peaks at 1630 cm^{-1} and 1750 cm^{-1}. The band near 1630 cm^{-1} is associated with sp^2 hybridized graphite, while the 1750 cm^{-1} is thought to originate from C=O functionality on the ND surface (*10*). These features are often observed in vibrational spectra of amorphous carbon samples that contain a high concentration of carbon atoms in mixed sp^2/sp^3 hybridization states (*11–13*). Since the most probable end product of a ND SBER type phase transition is graphite, a transition would be indicated in the Raman vibrational spectrum by a sharp increase in the sp^2 peak centered near 1630 cm^{-1}. The intensity of this feature in the RND spectrum remains fairly consistent over the pressure range studied, indicating that little to no transition occurs. This may be the result of thick amorphous carbon surface, as well as the sample impurities. However, in the OND spectra, there is a nearly two-fold intensity increase in the sp^2 feature that correlates well with the intensity increase of the 1260 cm^{-1} feature. This suggests that a partial phase transition from sp^3 hybridized diamond to sp^2 hybridized graphite may be occurring, but it is sluggish.

3.2 Theoretical

DFT calculations were used to characterize a bare, reconstructed ND composed of 2052 atoms; the optimized structure of this ND is shown in figure 2. The bonds within the core were analyzed by calculating the average distance from an atom to its four nearest neighbors. These averages were then binned and averaged by the distance of the atom from the center of the nanodiamond. These bond lengths were then compared to the bond lengths of bulk diamond to provide estimates of the internal pressure of the core by comparing local bond structure to that of bulk diamond at known pressure. Although the material near the surface is significantly distorted from that of bulk diamond (see the equilibrium configuration shown in figure 2), the material within the core has the same coordination and orientation of the bonds as bulk diamond, except that the bonds are compressed to a point that corresponds to 50 GPa in compressed bulk diamond. Thus, we estimate that the internal pressure is ~50 GPa.

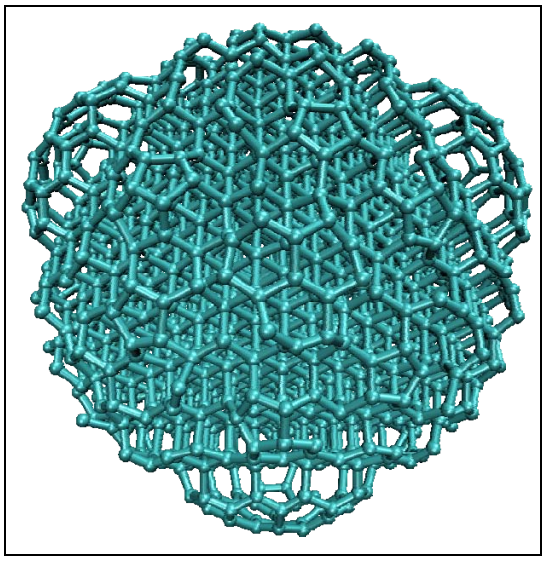

Figure 2. Equilibrated ND.

QMD simulations were then performed on two such bare, reconstructed ND subjected to hypervelocity non-central collisions in order to explore conditions in which the outer shells could be disrupted and the subsequent effect. The simulation involved an off-center high velocity collision of two NDs moving relative to one another at 20 km/s. Figure 3 shows a series of sequential snapshots of colliding NDs during this trajectory from two perspectives: the left-most frames show the NDs moving into or out of the plane of visualization; the right-most frame shows the NDs moving along the horizontal axis.

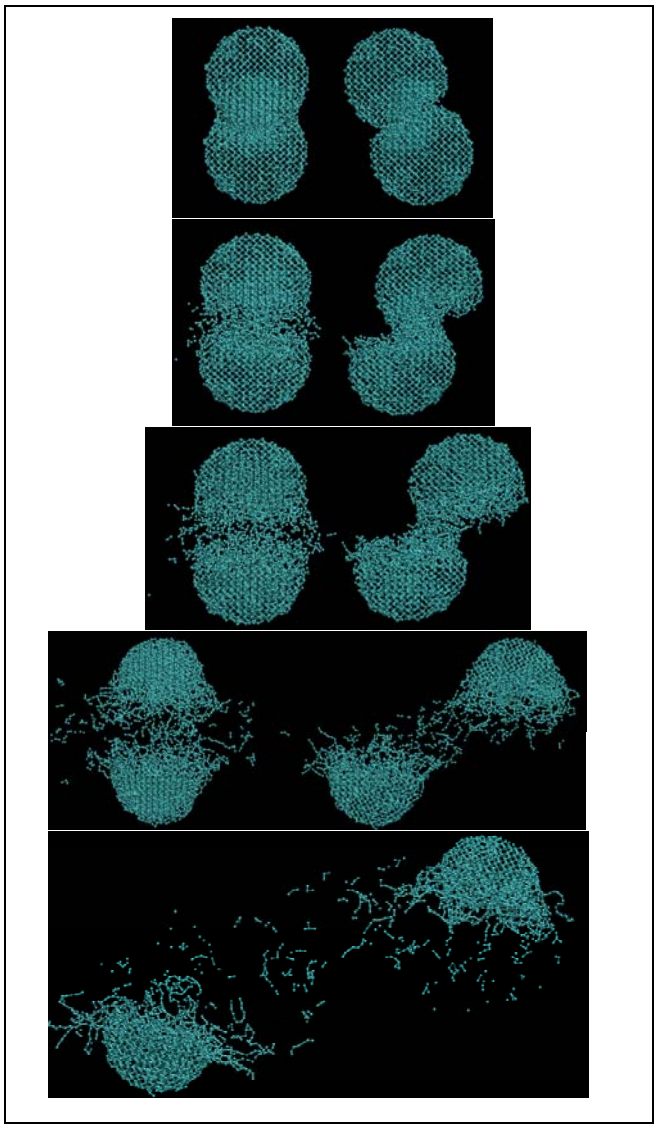

Figure 3. Snapshot of colliding NDs at 0.076 ps (top), 0.15 ps (second frame), 0.20 ps (third frame), 0.359 ps (fourth frame), 0.589 ps (bottom frame).

Note: All but the bottom frame show the collision from two perspectives. (See text).

Upon collision, shock waves propagate through the bodies of the NDs, and amorphization of the material at the contact region occurs as seen in first frame of figure 3 (t=0.076 ps). In the second frame of the snapshot at 0.15 ps, each ND shears and compresses material from the other in the region of the direct collision of the two particles, leading to a configuration of the two conjoined particles that resembles an "S". At t=0.20 ps (third frame), the two fragments separate, and we see the initial relaxation (expansion) of the region of the material that has been sheared and the ejection of small fragments (ranging from atoms to small carbon clusters) into the vacuum. The fourth frame, depicting the system at 0.359 ps, shows a continuing separation of the particles, with the various polyatomic moieties departing from the sheared region of the NDs into the

vacuum. The material at the sheared region of the fragments expands in all directions, leading to a deformation of the parent fragment. The bottom frame, corresponding to t=0.589 ps, shows that the fragments are continuing to expand and flatten relative to the original spherical shape. Additionally, the fragments are rotated relative to their initial arrangement about their inertial axes, indicating that during the collision, the fragments gain angular momentum. Animation of the snapshots for the duration of the trajectory shows that the atoms on the entire surface of the retreating fragments are mobile, and that the surface material appears unstable. We are further exploring the behavior of these retreating fragments, as well as exploring these collisions at lower relative collision velocities (10 and 5 km/s).

It is quite apparent from these simulations that high velocity collisions, indeed, disrupt the ND, which subsequently comminutes into mono- and multi-atomic fragments that are moving at high velocities and that are probably highly reactive. Such high-velocity reactive particles, when coming into contact with atmospheric gases, would result in combustion, thus providing significant energy release. We intend to introduce molecular oxygen into a subsequent series of simulations in order to explore this possibility.

4. Conclusions

The above theoretical results indicate that ND could be potential sources of SBE for potential use as next-generation energetic materials; however, the key to its use appears to be in the sudden rupture of the surface. Unlike the idealized ND explored in our theoretical study, nanodiamond particles produced by detonation synthesis have a composite structure comprised of a diamond core and an amorphous carbon outer shell. The outer shell thickness can be modified through various purification schemes, and it is reasonable to expect variations in the SBER potential of nanodiamonds prepared under differing purification methods. Static high-pressure Raman spectroscopic measurements collected to 53 GPa showed a slight intensity increase in the OND feature near 1335 cm^{-1}, which lies within the partial density of states of the diamond lattice. The intensification of this vibrational feature is consistent with a thinner amorphous carbon outer shell, which results in greater exposure to the diamond core under subsequent pressure increases. Exposure of the diamond core is thought to be an important precursor to SBER initiation. Additionally, a nearly two-fold increase in the vibrational intensity of the sp^2 graphite peak centered near 1630 cm^{-1} in the OND spectrum suggests the possibility of a sluggish partial phase transition from sp^3-hybridized diamond to sp^2-hybridized graphite. Future experiments will focus on combining high-pressure with high-shear/strain conditions to judge whether the SBER phenomena can be triggered in nanodiamond materials. We expect that further theoretical and experimental investigations into the surface morphology and requirements to crack the shell will allow for a fundamental understanding of the conditions in which rapid release of this energy can be used.

5. References

1. Bridgman, P. W. Effects of High Shearing Stress Combined with High Hydrostatic Pressure. *Phys. Rev.* **1935**, *48*, 825.

2. Al'tschuler, A. M. *Structural Bond Energy Release as a New Propagation Mechanism of Explosive, Chemical and Nuclear Reactions*; Technical Report TRC-90-001; Technical Research Corporation, McLean, VA, 1990.

3. Al'tschuler, A. M. *Structural Bond Energy Release in Energetic Materials as New Means for Designing Nonconventional High Explosives: An Analysis of Soviet Research*; Technical Report TRC-91-003; Technical Research Corporation, McLean, VA, 1991.

4. Raty, J. Y.; Galli, G.; Bostedt, C.; van Buren, T. W.; Terminello, L. J. Quantum Confinement and Fullerenelike Surface Reconstructions in Nanodiamonds. *Phys. Rev. Lett.* **2003**, *90*, 037401.

5. Romero, N. A.; Mattson, W. D. Density Functional Calculation for the Shock Hugoniot of Diamond. *Phys. Rev. B* **2007**, *76*, 214113.

6. Zha, C. S.; Mao, H. K.; Hemley, R. J., Elasticity of MgO and a Primary Pressure Scale to 55 GPa. *Proc. Nat. Acad. Sci,* **2000**, *97*, 13494.

7. Goncharov, A. F.; Hemley, R. J.; Mao, H. K.; Shu, J. New High-Pressure Excitations in Parahydrogen. *Phys. Rev. Lett.* **1998**, *80*, 101.

8. Yoshikawa, M.; Mori, Y.; Maegawa, M.; Katagiri, G.; Ishida, H.; Ishitani, A. Raman Scattering from Diamond Particles. *Appl. Phys. Lett.* **1993**, *62*, 3114.

9. Bachmann, P. K.; Bausen, H. D.; Lade, H.; Leers, D.; Wiechert, D. U.; Herres, N.; Kohl, R.; Koidl, P. Raman and X-ray Studies of Polycrystalline CVD Diamond Films. *Diam. Relat. Mater.*, **1994**, *3*, 1308.

10. Mykhaylyk, O. O.; Solonin, Y. M.; Batchelder, D. N.; Brydson, R. Transformation of Nanodiamond into Carbon Onions. *J. Appl. Phys.*, **2005**, *97*, 074302.

11. Ferrari, A. C.; Robertson, J. Resonant Raman Scattering of Disordered, Amorphous and Diamond-like Carbon. *Phys. Rev. B*, **2001**, *64*, 075414.

12. Gilkes, K.W.R.; Sands, H. S.; Batchelder, D. N.; Robertson, J.; Milne, W. I.. Direct Observation of sp^3 Bonding in Tetrahedral Amorphous Carbon using Ultraviolet Raman Spectroscopy. *Appl. Phys. Lett.* **1997**, *70*, 1980.

13. Merkulov, V. I.; Lannin, J. S.; Munro, C. H.; Asher, S. A.; Veerasamy, V. S.; Milne, W.I. UV studies of Tetrahedral Bonding in Diamondlike Amorphous Carbon. *Phys. Rev. Lett.* **1997**, *78*, 4869.

List of Symbols, Abbreviations, and Acronyms

ARL	U.S. Army Research Laboratory
DFT	Density Functional Theory
DoD	Department of Defense
FSU	former Soviet Union
GGA	Generalized Gradient Approximation
NDs	nanodiamonds
OND	Oxidized
QMD	Quantum Molecular Dynamics
RESPA	reference system propagator algorithm
RND	Raw
SBER	Structural Bond Energy Release
SC	single crystal

NO. OF COPIES	ORGANIZATION
1 (PDF ONLY)	DEFENSE TECHNICAL INFORMATION CTR DTIC OCA 8725 JOHN J KINGMAN RD STE 0944 FORT BELVOIR VA 22060-6218
1 CD	DIRECTOR US ARMY RESEARCH LAB IMNE ALC HRR 2800 POWDER MILL RD ADELPHI MD 20783-1197
1 CD	DIRECTOR US ARMY RESEARCH LAB AMSRD ARL CI OK TL 2800 POWDER MILL RD ADELPHI MD 20783-1197
1 CD	DIRECTOR US ARMY RESEARCH LAB AMSRD ARL CI OK PE 2800 POWDER MILL RD ADELPHI MD 20783-1197
2	COMMANDER US ARMY RSRCH OFC TECH LIB R ANTHENIAN PO BOX 12211 RESEARCH TRIANGLE PARK NC 27709-2211
1	DIRECTOR US ARMY RSRCH LAB AMSRD ARL RO P TECH LIB PO BOX 12211 RESEARCH TRIANGLE PARK NC 27709-2211
4	COMMANDER NAVAL RSRCH LAB TECH LIB CODE 4410 K KAILASANATE J BORIS E ORAN 4555 OVERLOOK AVE NW WASHINGTON DC 20375-5000
1	OFFICE OF NAVAL RSRCH J GOLDWASSER 975 N RANDOLPH ST RM 653 ARLINGTON VA 22217-5000
1	COMMANDER NAWC INFO SCI DIV CHINA LAKE CA 93555-6001
2	COMMANDER NAWC CODE 3895 CH1NA LAKE CA 93555-6001
1	WL MNME ENERGETIC MTRL BR 2306 PERIMETER RD STE 9 EGLIN AFB FL 32542-5910
1	DIRECTOR SANDIA NATL LAB M BAER DEPT 1512 PO BOX 5800 ALBUQUERQUE NM 87185
2	DIRECTOR LLNL ALFRED BUCKINGHAM L 023 MILTON FINGER L 020 PO BOX 808 LIVERMORE CA 94550-0622
1	CIA J BACKOFEN RM 4PO7 NHB WASHINGTON DC 20505
2	SRI INTRNTL TECH LIB PROPULSION SCI DIV 333 RAVENWOOD AVE MENLO PARK CA 94025-3493
1	RDECOM ARDEC TECH LIB BLDG 59 PICATINNY ARSENAL NJ 07806-5000

NO. OF COPIES	ORGANIZATION
1	AIR FORCE RSRCH LAB MNME EN MAT BR B WILSON 2306 PERIMETER RD EGLIN AFB FL 32542-5910
1	AIR FORCE OFC OF SCI RSRCH M BERMAN 875 N RANDOLPH ST STE 235 RM 3112 ARLINGTON VA 22203-1768
2	LLNL TECH/INFO DEPT LIB PO BOX 808 LIVERMORE CA 94550-0622
2	LOS ALAMOS NATL LAB TECH LIB MS-P362 PO BOX1663 LOS ALAMOS NM 87545-1362
3	NIST CENTER FOR NEUTRON RESEARCH T JENKINS 100 BUREAU DR MS8562 GAITHERSBURG MD 20899

NO. OF COPIES	ORGANIZATION
ABERDEEN PROVING GROUND	
16	DIR USARL AMSRD ARL WM B M ZOLTOSKI AMSRD ARL WM BD R BEYER E BYRD B FORCH J CIEZAK (3 CPS) K MCNESBY M MCQUAID R PESCE-RODRIGUEZ B RICE AMSRD ARL WM M S MCKNIGHT AMSRD ARL WM SG T ROSENBERGER AMSRD ARL WM T B BURNS P BAKER AMSRD ARL WM TD D DANDEKAR
1 CD	DIR USARL AMSRD ARL CI OK TP (BLDG 4600)
TOTAL:	48 (1 elec, 4 CDs, 43 HCs)